Development of a Hybrid Actuation System for Haptic Interfaces

Carlos Rossa

University of Paris VI
&
French Atomic Energy Commission

January 15th 2014

Schematic representation of a haptic interaction

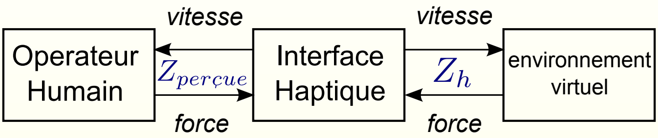

- Ideal haptic interface :

$$\frac{Z_{perçue}}{Z_h} = 1$$

- Free motion ($Z_h \to 0$) : no inertia and no friction
- Virtual obstacle ($Z_h \to \infty$) : infinite output impedance

Actives Interfaces

Schematic representation of a haptic interaction

Advantages

- Allow for energy dissipation and restitution
- Low response time
- Relatively good control performance

Drawbacks

- Low torque per volume unit
- Need reduction stages
- Low efficiency

Actives Interfaces

Schematic representation of a haptic interaction

Advantages

- Allow for energy dissipation and restitution
- Low response time
- Relatively good control performance

Drawbacks

- Low torque per volume unit
- Need reduction stages
- Low efficiency

Active interface drawbacks

Simplified model of a haptic interaction using an active actuator

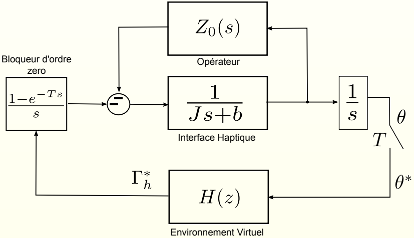

- Simulation of a virtual wall with stiffness K and damping B :

Active interface drawbacks

Simplified model of a haptic interaction using an active actuator

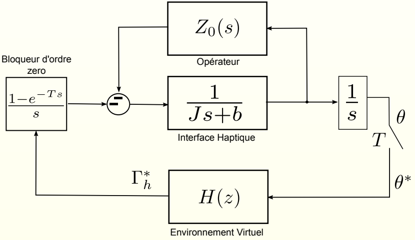

- Simulation of a virtual wall with stiffness K and damping B :

$$b > \frac{KT}{2} + B$$

[Colgate 94]

Passive Interfaces

Simplified model of a haptic interaction using a passive actuator

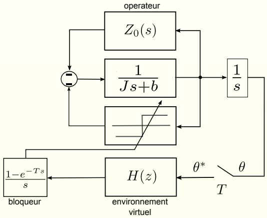

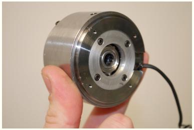

There is no limit for the control gains of $H(z)$

- Low power consumption
- High torque per volume ratio

Passive Interfaces

Simplified model of a haptic interaction using a passive actuator

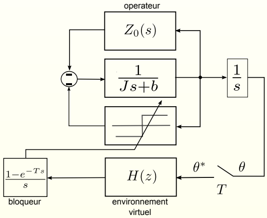

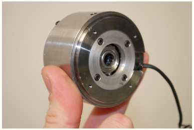

There is no limit for the control gains of $H(z)$

- Low power consumption
- High torque per volume ratio

Passive Interfaces

Simplified model of a haptic interaction using a passive actuator

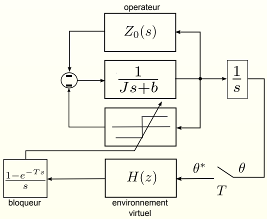

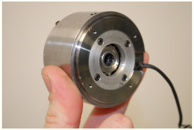

There is no limit for the control gains of $H(z)$

- Low power consumption
- High torque per volume ratio

Cannot restore energy to the operator

Passive Interfaces Drawbacks

- Impossibility to restore energy

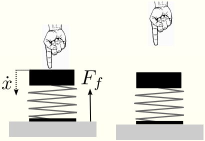

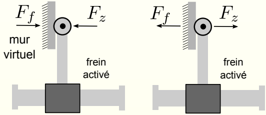

- Force control in MDOF

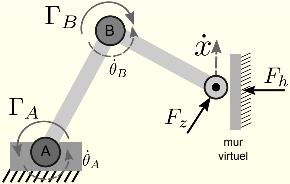

Hybrid Interfaces

- The brake imposes a controllable damping

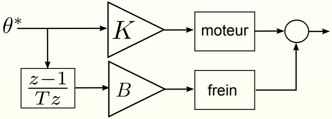

$$b + B > \frac{KT}{2}$$

- The motor compensates for the viscous friction

- **Proposed approach** :

Hybrid Interfaces

- The brake imposes a controllable damping

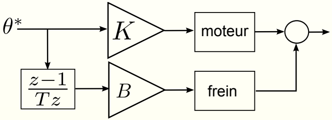

$$b + B > \frac{KT}{2}$$

- The motor compensates for the viscous friction

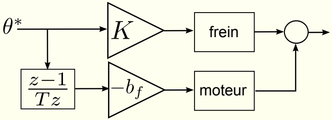

$$b_f < b$$

- Proposed approach :

Hybrid Interfaces

- The brake imposes a controllable damping

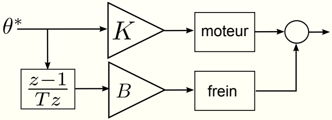

$$b + B > \frac{KT}{2}$$

- The motor compensates for the viscous friction

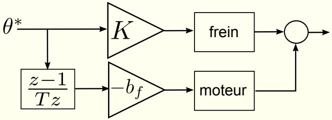

$$b_f < b$$

- **Proposed approach** :

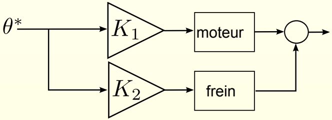

$$K = K_1 + K_2$$

$$K_1 < \frac{2b}{T}$$

Brake/motor parallel systems

Indetermination at zero speed

1. The operator has resealed the end-effector
2. Force equilibrium

If $|F_f| > |F_m|$:

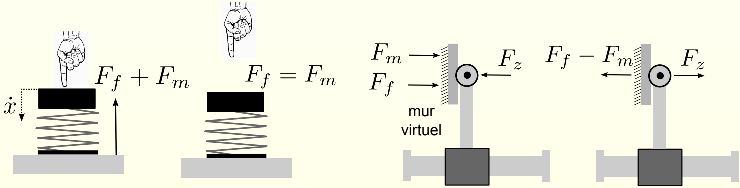

C. Rossa *et al.* - Interaction power flow based control of a 1-DOF hybrid haptic interface - Eurohaptics 2012

Proposed Approach

Mechanical constraints

The brake does not block the motor
Unidirectional brakes
Integrated design

Control constraints

Control in impedance loop without a measure of torque
Control laws independent of the virtual environment
Limitation of the control loop gains

Proposed Approach

Mechanical constraints

The brake does not block the motor
Unidirectional brakes
Integrated design

Control constraints

Control in impedance loop without a measure of torque
Control laws independent of the virtual environment
Limitation of the control loop gains

The Hybrid Actuation system

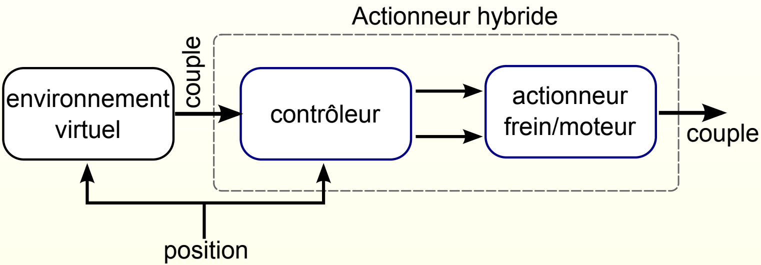

Actuation system independent of any application

Presentation outline

Sommaire

Working principle of unidirectional brakes

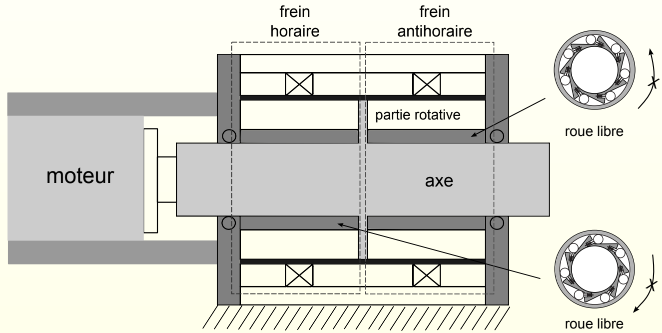

C. Rossa, J. Lozada and A. Micaelli - Actuator with hybrid actuation for a force feedback interface - Patent WO-A1, 2012

Working principle of unidirectional brakes

1. "Sticky wall" avoidance

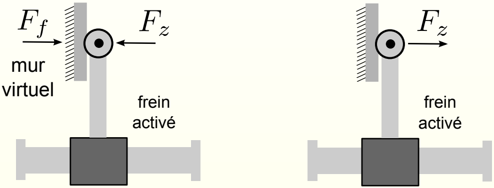

2. The imposed torque has always the sign of the desired torque

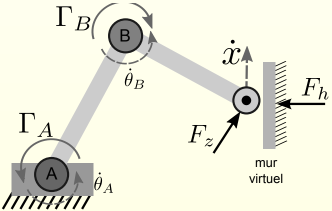

C. Rossa *et al.* - A new hybrid actuator approach for force-feedback devices - IROS 2012

Sommaire

Magnetorheological fluids (MR)

- Rheological effect in a fluid suspension

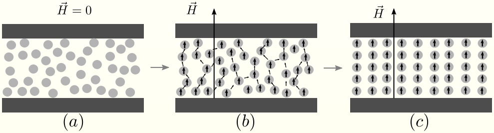

- Bingham viscoelastic model :

$$|\tau(\dot{\gamma}, H)| = \tau_y(H) + \eta|\dot{\gamma}|$$

τ	yield stress	$\dot{\gamma}$	shear rate
H	magnetic field	η	viscosity
τ_y	field dependent yield stress		

C. Rossa *et al.* - Magnetic flux analysis on MR actuators can detect external force variation - IEEE Sensors Conference 2012

C. Rossa *et al.* - On a novel torque detection technique for MR actuators - IEEE Sensors Journal 2013

Magnetorheological fluids

- Modification of the fluid's apparent viscosity

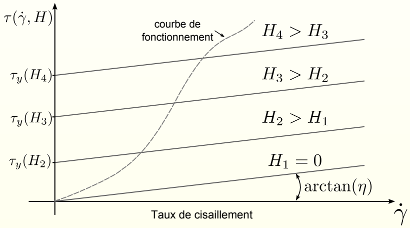

- Ideal behaviour ($\dot{\gamma} = 0$ if $\tau < \tau_y$)
- Direct shear operation mode :

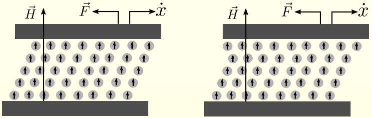

Elementary rotary MR brakes

- Rotary brakes based on the direct shear mode :

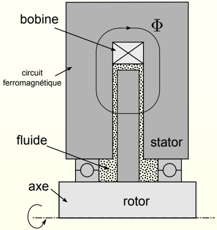

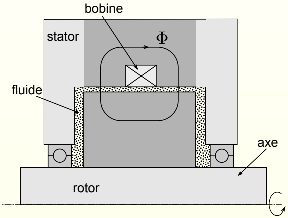

- The torque is given by :

$$|\Gamma(H,\dot{\gamma})| = \int\int R|\tau(H,\dot{\gamma})|dS$$

Proposed magnetostatic model

gap

Fluide

Surface
(type de frein)

Induction nominale

matériau circuit mag

- Clt. Torque/volume
- Clt. Torque/power
- Clt. Torque/time cons
- Clt. Torque/Visc. Torque

C. Rossa *et al.* - Design Considerations for Magnetorheological Brakes - Transactions on Mechatronics IEEE/ASME 2013

Proposed magnetostatic model

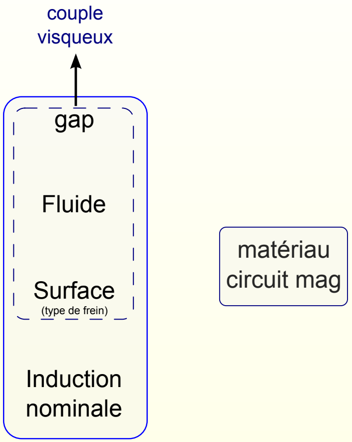

- Clt. Torque/volume
- Clt. Torque/power
- Clt. Torque/time cons
- Clt. Torque/Visc. Torque

C. Rossa *et al.* - Design Considerations for Magnetorheological Brakes - Transactions on Mechatronics IEEE/ASME 2013

Proposed magnetostatic model

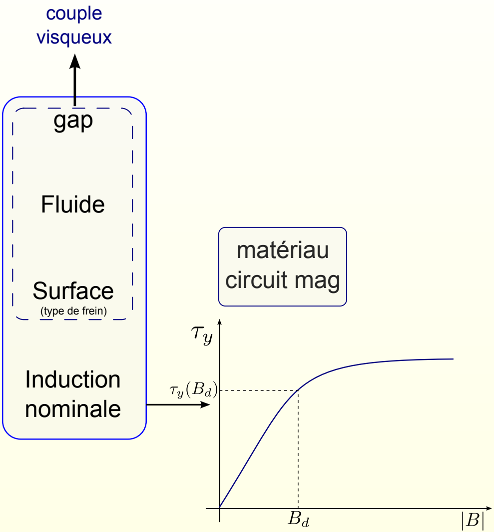

- Clt. Torque/volume
- Clt. Torque/power
- Clt. Torque/time cons
- Clt. Torque/Visc. Torque

C. Rossa *et al.* - Design Considerations for Magnetorheological Brakes - Transactions on Mechatronics IEEE/ASME 2013

Proposed magnetostatic model

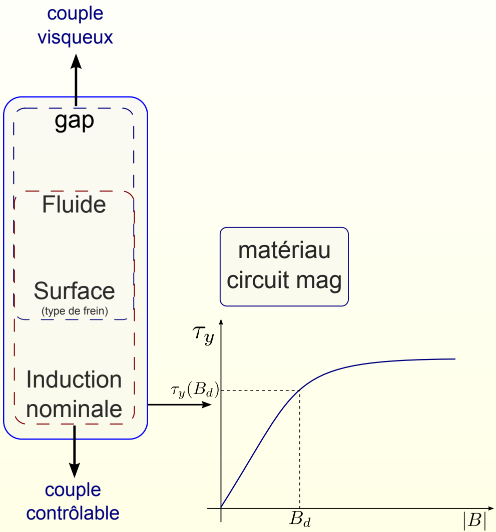

- Clt. Torque/volume
- Clt. Torque/power
- Clt. Torque/time cons
- Clt. Torque/Visc. Torque

C. Rossa *et al.* - Design Considerations for Magnetorheological Brakes - Transactions on Mechatronics IEEE/ASME 2013

Proposed magnetostatic model

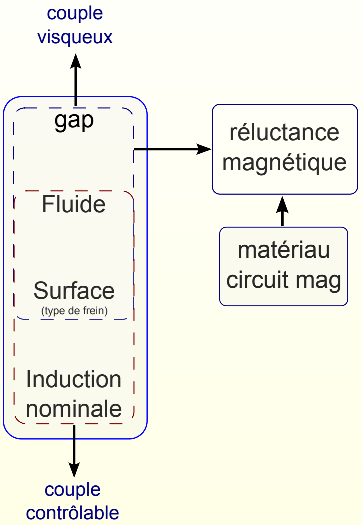

- Clt. Torque/volume
- Clt. Torque/power
- Clt. Torque/time cons
- Clt. Torque/Visc. Torque

C. Rossa *et al.* - Design Considerations for Magnetorheological Brakes - Transactions on Mechatronics IEEE/ASME 2013

Proposed magnetostatic model

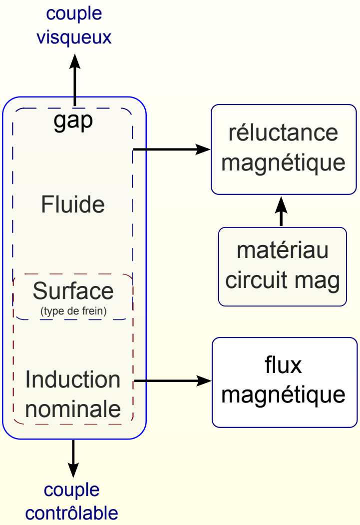

- Clt. Torque/volume
- Clt. Torque/power
- Clt. Torque/time cons
- Clt. Torque/Visc. Torque

C. Rossa *et al.* - Design Considerations for Magnetorheological Brakes - Transactions on Mechatronics IEEE/ASME 2013

Proposed magnetostatic model

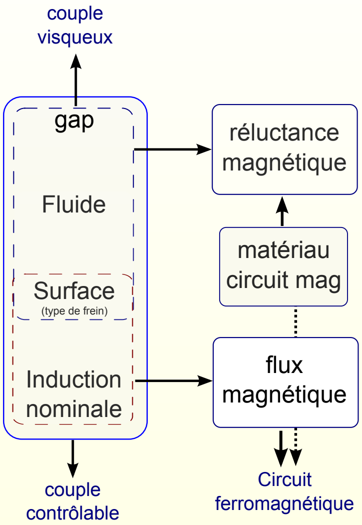

- Clt. Torque/volume
- Clt. Torque/power
- Clt. Torque/time cons
- Clt. Torque/Visc. Torque

C. Rossa *et al.* - Design Considerations for Magnetorheological Brakes - Transactions on Mechatronics IEEE/ASME 2013

Proposed magnetostatic model

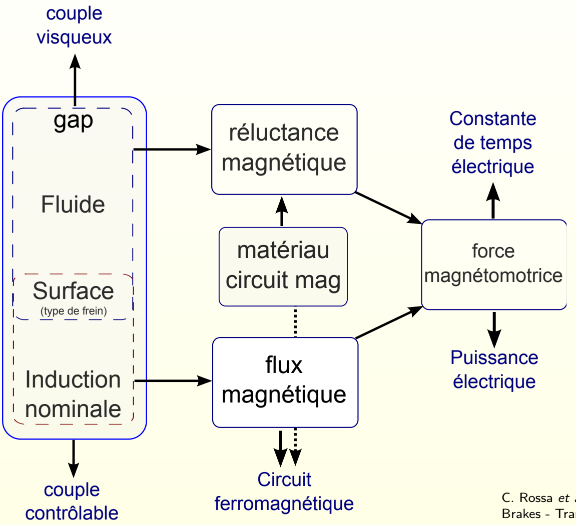

- Clt. Torque/volume
- Clt. Torque/power
- Clt. Torque/time cons
- Clt. Torque/Visc. Torque

C. Rossa *et al.* - Design Considerations for Magnetorheological Brakes - Transactions on Mechatronics IEEE/ASME 2013

Proposed magnetostatic model

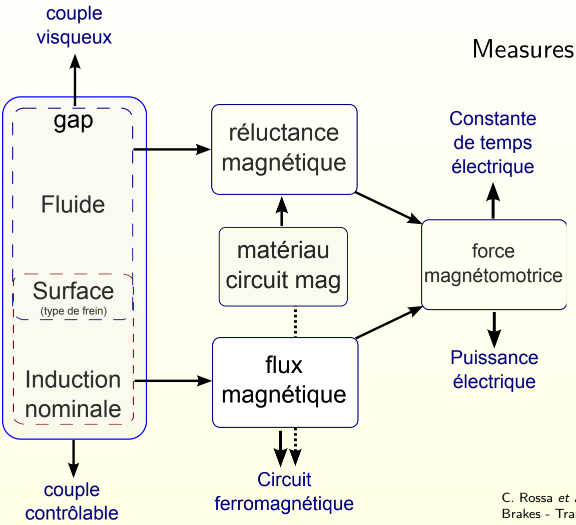

Measures of performance :

- Clt. Torque/volume
- Clt. Torque/power
- Clt. Torque/time cons
- Clt. Torque/Visc. Torque

C. Rossa *et al.* - Design Considerations for Magnetorheological Brakes - Transactions on Mechatronics IEEE/ASME 2013

Mutilayered brakes

Multiple discs brake

- Additional parameter
- Equivalent surfaces

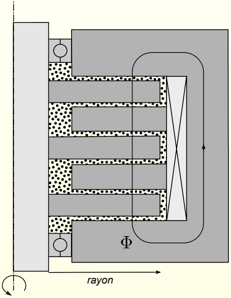

Multiple cylinders brake

- Nonlinear model
- Desired induction specified across the smallest surface

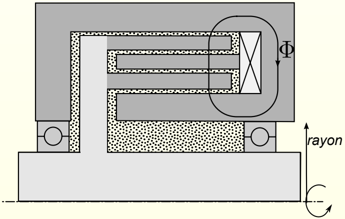

Sommaire

Brake design

- Design constraints
  - Desired torque 3.2 Nm
  - Hollow shaft
  - Gap 0.5 mm
- Magnetic Saturation
  - Iron maximum induction 1.7 T
  - Fluid maximum induction 0.7 T
- Optimization variables
  - Number of fluid gaps
  - Length of fluid gaps
  - Inner radius
  - Coil radius
- Cost functions

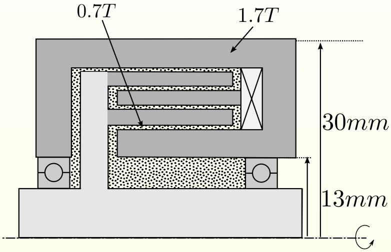

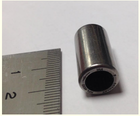

C. Rossa *et al.* - Development of a multilayered wide-ranged magnetorheological brake - Smart Materials and Structures 2014

Brake design

- Design constraints
  - Desired torque 3.2 Nm
  - Hollow shaft
  - Gap 0.5 mm
- Magnetic Saturation
  - Iron maximum induction 1.7 T
  - Fluid maximum induction 0.7 T
- Optimization variables
  - Number of fluid gaps
  - Length of fluid gaps
  - Inner radius
  - Coil radius
- Cost functions

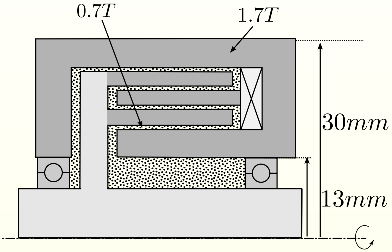

C. Rossa *et al.* - Development of a multilayered wide-ranged magnetorheological brake - Smart Materials and Structures 2014

Brake design

- Design constraints
  - Desired torque 3.2 Nm
  - Hollow shaft
  - Gap 0.5 mm
- Magnetic Saturation
  - Iron maximum induction 1.7 T
  - Fluid maximum induction 0.7 T
- Optimization variables
  - Number of fluid gaps
  - Length of fluid gaps
  - Inner radius
  - Coil radius
- Cost functions

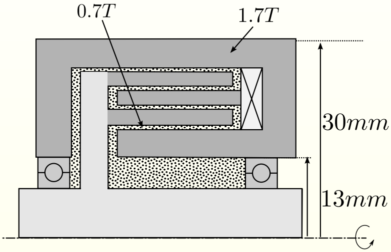

C. Rossa *et al.* - Development of a multilayered wide-ranged magnetorheological brake - Smart Materials and Structures 2014

Brake design

- Design constraints
  - Desired torque 3.2 Nm
  - Hollow shaft
  - Gap 0.5 mm
- Magnetic Saturation
  - Iron maximum induction 1.7 T
  - Fluid maximum induction 0.7 T
- Optimization variables
  - Number of fluid gaps
  - Length of fluid gaps
  - Inner radius
  - Coil radius
- Cost functions

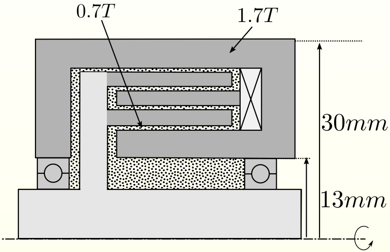

$$\min \left(\frac{torque - 3.2Nm}{3.2Nm} \right)$$

$$\max \left(\frac{torque}{volume} \right)$$

C. Rossa *et al.* - Development of a multilayered wide-ranged magnetorheological brake - Smart Materials and Structures 2014

Final characteristics

- Optimization results

Number of gaps	4
Gap length	7 mm
Outer radius	30 mm
Total length	39 mm

- According to the analytical model :

Viscous friction	0.324 mNms

Final characteristics

- Optimization results

Number of gaps	4
Gap length	7 mm
Outer radius	30 mm
Total length	39 mm

- According to the analytical model :

Viscous friction	0.324 mNms

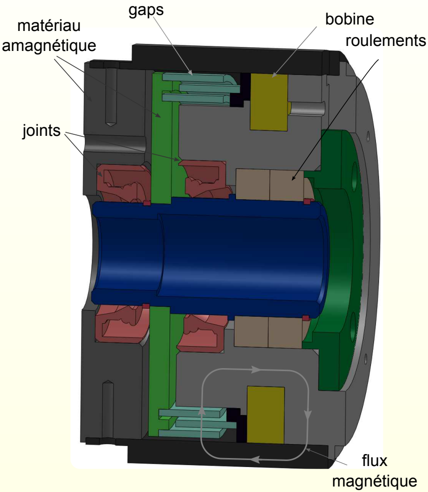

Finite element analysis

- Coil wire turns : 475
- 0.7 T across the fluid surface requires :
  - According to FEM : 0.52 A
  - According to the analytical model : 0.49 A

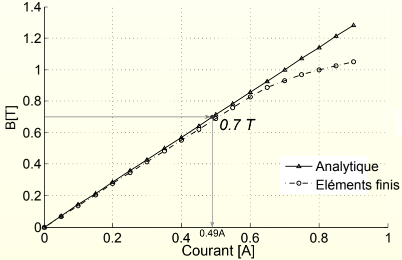

Finite element analysis

- Coil wire turns : 475
- 0.7 T across the fluid surface requires :
  - According to FEM : 0.52 A
  - According to the analytical model : 0.49 A

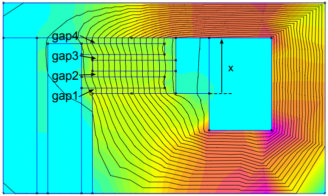

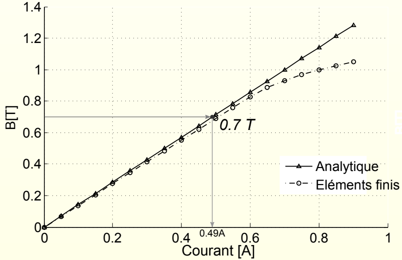

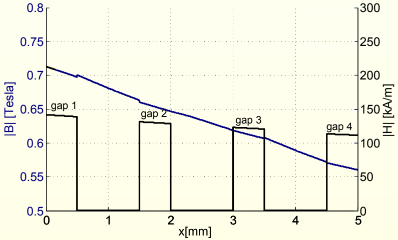

Unidirectional brakes

CAD of the brakes

Different parts that compose a brake

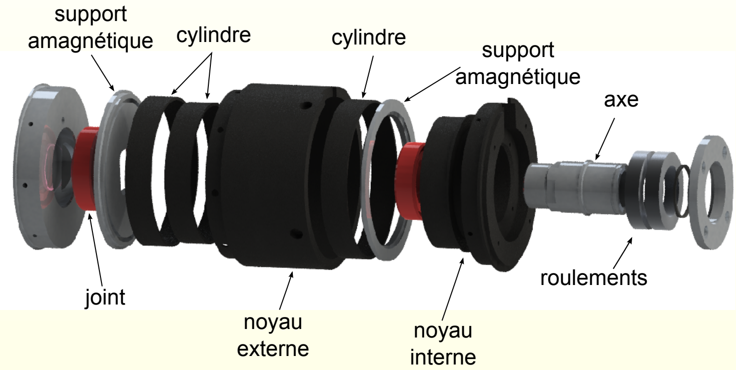

Characterization

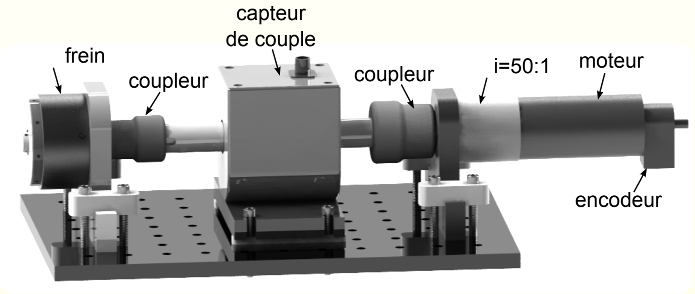

Mechanical characteristics

- Torque at 0.49 A : 3.6 Nm (+5.5%)
- Maximal torque : 5.3 Nm
- Coulomb friction : 30 mNm

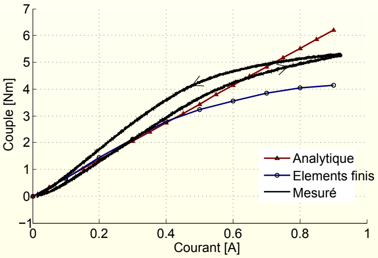

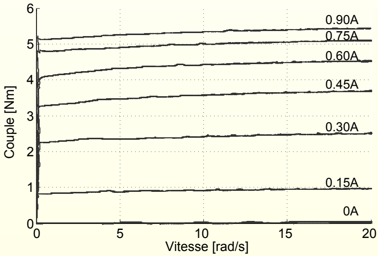

Performance evaluation

Performance evaluation

	unit	proposed brake	LordCorp RD2078	Senkal et al.	Nam et al.
Torque Max	Nm	5.3	4.0	10.9	4.2
Torque Min	mNm	30	400	100	-
L/R	mm	39/30	35/96	89/32	38/60
Power	W	19	15	20	52
Time cte	ms	50	10	60	33
Torque/Vol	kN/m^2	48.1	12.5	38.3	9.8
power/torq	mNm/W	280	260	540	80
Max/Min.	-	176	10	109	-
time/torq	kNm/s	106	400	108	127

Cross view of the hybrid actuator

- Two identical brakes and a motor compose the actuator
- DC Maxon motor RE40 (220 mNm)

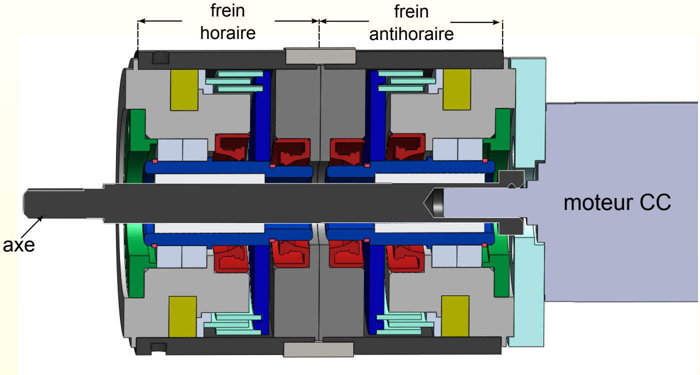

Sommaire

Block diagram

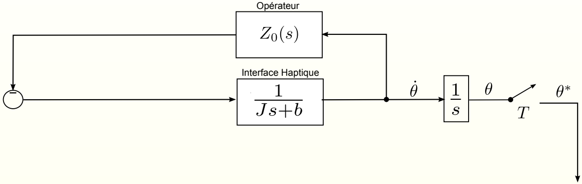

Block diagram

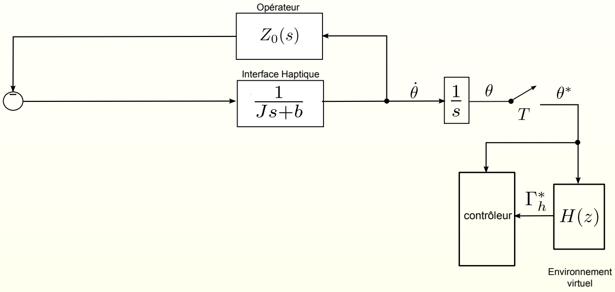

Block diagram

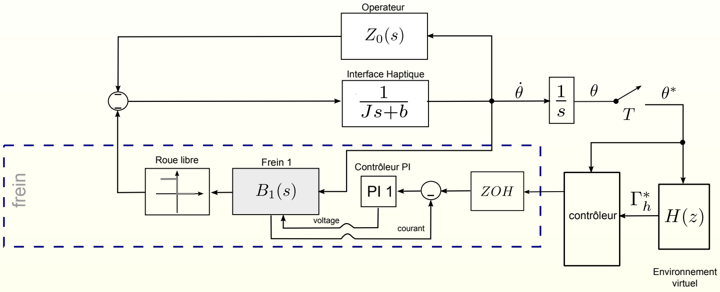

Block diagram

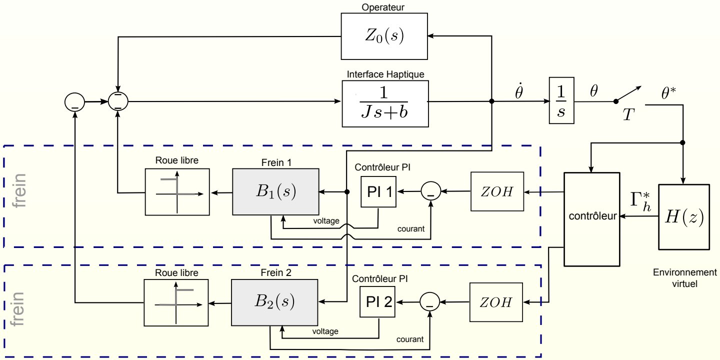

Block diagram

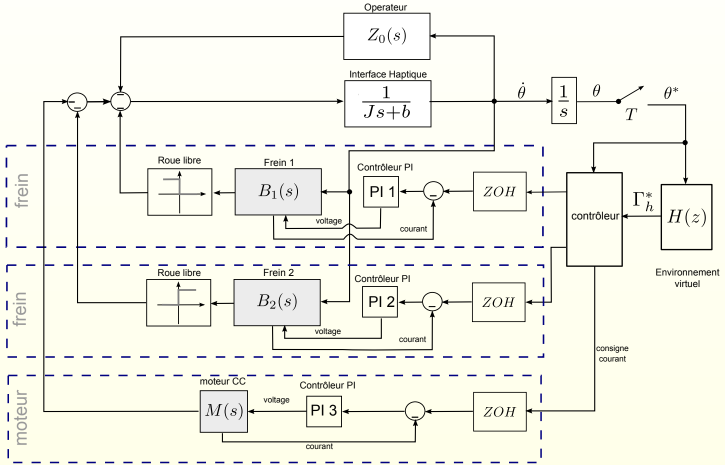

Block diagram

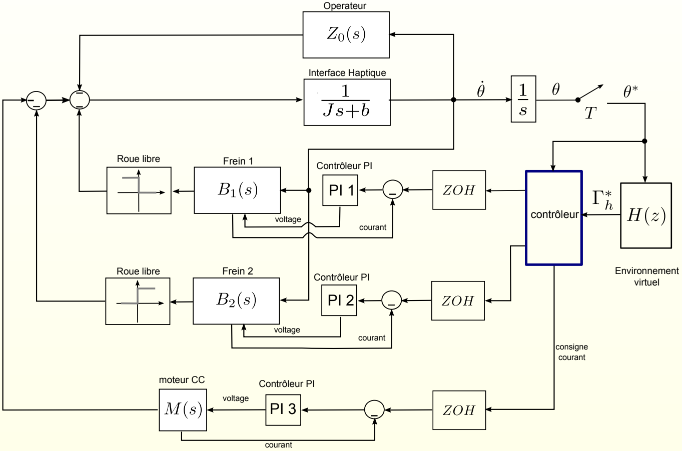

Control premise

Only two input variables :

- The desired torque
- The measured position

Elements to be taken into account :

1. The maximal gain for the motor is :

$$K_{lim} < \frac{2b}{T}$$

2. Follow a reference torque using the motor/brake
3. Active torque Γ_{sat} 0.2 Nm
4. Passive torque 5.3 Nm

Limitation of the motor's stiffness

The desired stiffness K_h is :

$$K_{h(k)} = \frac{\Gamma_{h(k)} - \Gamma_{sb(k-1)}}{\delta\theta}$$

- Γ_h reference torque, Γ_{sb} motor's torque, $\delta\theta$ position variation

The torque imposed by motor is :

1. If K_h is inferior to K_{lim}

$$\Gamma_{sb(k)} = \Gamma_{h(k)}$$

2. Otherwise $K_h > K_{lim}$; thus :

$$\Gamma_{sb(k)} = K_{lim}.\delta\theta + \Gamma_{sb(k-1)}$$

C. Rossa *et al.* - Stable haptic interaction using passive and active actuators - ICRA 2013

Limitation of the motor's stiffness

The desired stiffness K_h is :

$$K_{h(k)} = \frac{\Gamma_{h(k)} - \Gamma_{sb(k-1)}}{\delta\theta}$$

- Γ_h reference torque, Γ_{sb} motor's torque, $\delta\theta$ position variation

The torque imposed by motor is :

1. If K_h is inferior to K_{lim}

$$\Gamma_{sb(k)} = \Gamma_{h(k)}$$

2. Otherwise $K_h > K_{lim}$; thus :

$$\Gamma_{sb(k)} = K_{lim}.\delta\theta + \Gamma_{sb(k-1)}$$

C. Rossa *et al.* - Stable haptic interaction using passive and active actuators - ICRA 2013

Limitation of the motor's stiffness

The desired stiffness K_h is :

$$K_{h(k)} = \frac{\Gamma_{h(k)} - \Gamma_{sb(k-1)}}{\delta\theta}$$

- Γ_h reference torque, Γ_{sb} motor's torque, $\delta\theta$ position variation

The torque imposed by motor is :

1. If K_h is inferior to K_{lim}

$$\Gamma_{sb(k)} = \Gamma_{h(k)}$$

2. Otherwise $K_h > K_{lim}$; thus :

$$\Gamma_{sb(k)} = K_{lim}.\delta\theta + \Gamma_{sb(k-1)}$$

C. Rossa *et al.* - Stable haptic interaction using passive and active actuators - ICRA 2013

Activation of the brake

Torque sharing coefficient :

$$\beta = \frac{min\left(|\Gamma_{sb}|, |\Gamma_{sat}|\right)}{|\Gamma_h|}$$

with Γ_{sat} the torque capability of the motor

$$\Gamma_{motor} = \beta.\Gamma_h$$

$$\Gamma_{brake} = (1-\beta).\Gamma_h$$

The brake is turned off if the torque and the velocity have same signs

Brake/motor activation

Simulation of a virtual angular spring

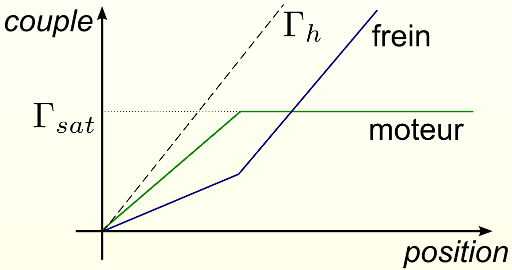

Experimental results

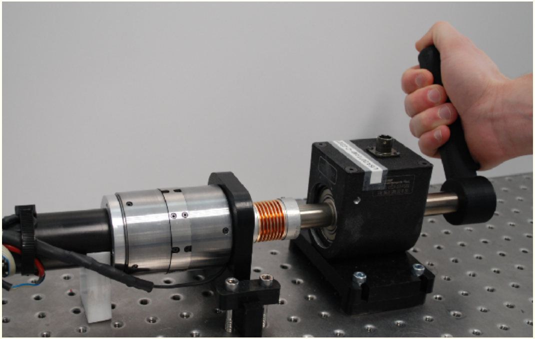

Experimental results - Brakes only

- 29 kNm/rad stiff virtual wall
- Obstacle at ± 0.1 rad

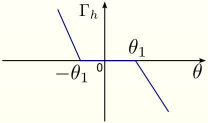

- Couple calculé par le contrôleur

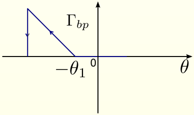

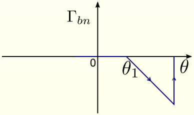

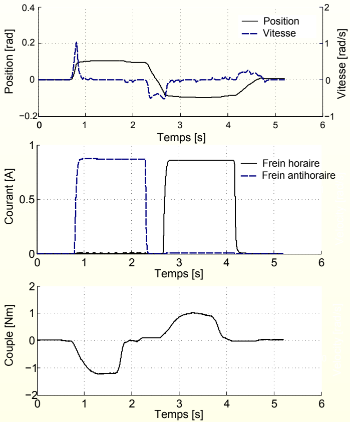

- Only the brake able to deliver Γ_h is activated

Experimental results - Angular spring

- Maximal gain of the motor 6.8 Nm/rad

Stiffness 6.8 Nm/rad

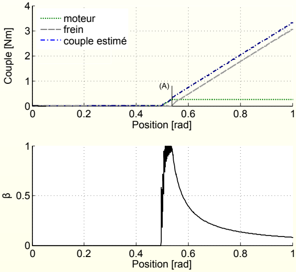

Stiffness 60 Nm/rad

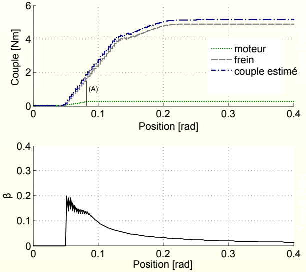

Experimental results - Angular spring

- Maximal gain of the motor 6.8 Nm/rad

Stiffness 6.8 Nm/rad

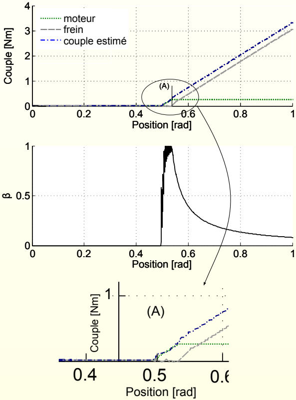

Stiffness 60 Nm/rad

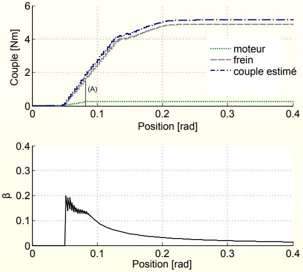

Experimental results - Angular spring

- Maximal gain of the motor 6.8 Nm/rad

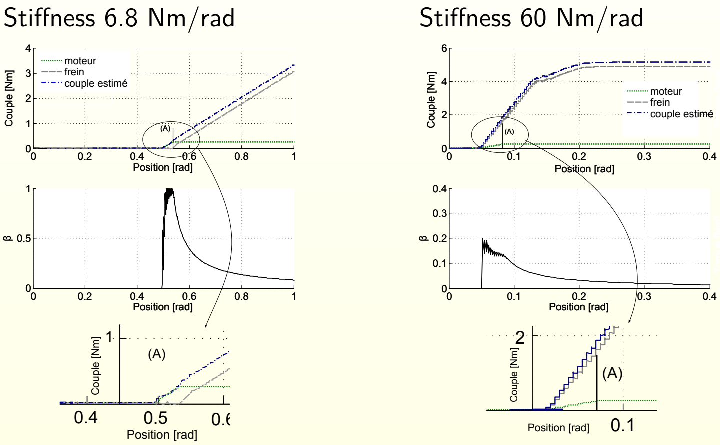

Hybrid actuator evaluation

- The passive torque is 27.5 times higher than the active torque
- Comparison with a motor with ideal capstan transmission

	Motor	Motor with capstan	Brake	Hybrid actuator	unit
Passive torque	0.2	5.5	5.3	5.5	Nm
Active torque	0.2	5.5	0	**0.2**	Nm
Réduction	1	27.5	1	1	-
Power	150	150	20	170	W
Inertia	134	101k	279	418	gcm^2
Viscous fric	5.24	144	567	732	μNms
Min torque	4.16	114.4	25.8	30	mNm
Torque/vol	2.24	-	48.1	17.75	kN/m^2

- Less friction up to 22.7 rev/s

Sommaire

Torque and stiffness asymmetry

Simulation of an angular spring

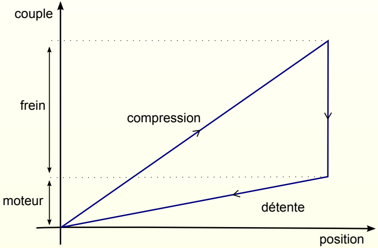

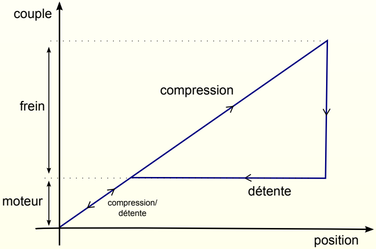

- Asymmetry due to the stiffness K_{lim} limitation
- Asymmetry due to the torque Γ_{sat} limitation

Methods

The motor is linked to a 7 :1 capstan transmission (max 1.2 Nm)

11 asymmetry levels	0%, 10%... 100%
2 stiffness levels	4.5 et 2.9 Nm/rad
2 maximal displacement	15° et 30°

(4 environments)x(11 levels)x(10 times)x(8+9 subjects) $=$ 7480

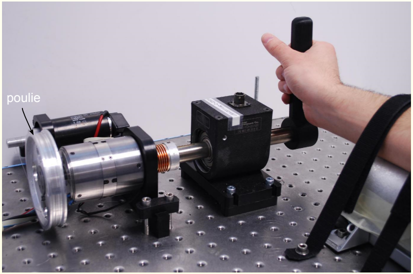

Results

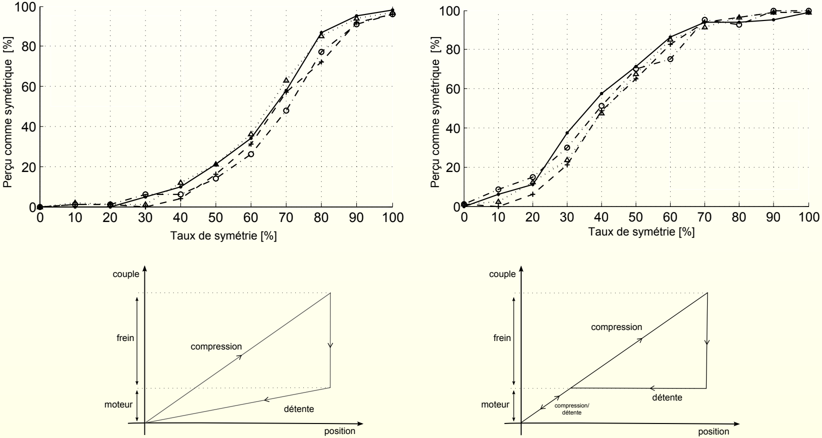

C. Rossa *et al.* - Perceptual evaluation of the passive/active torque and stiffness asymmetry of hybrid haptic device - Eurohaptics 2014

Results

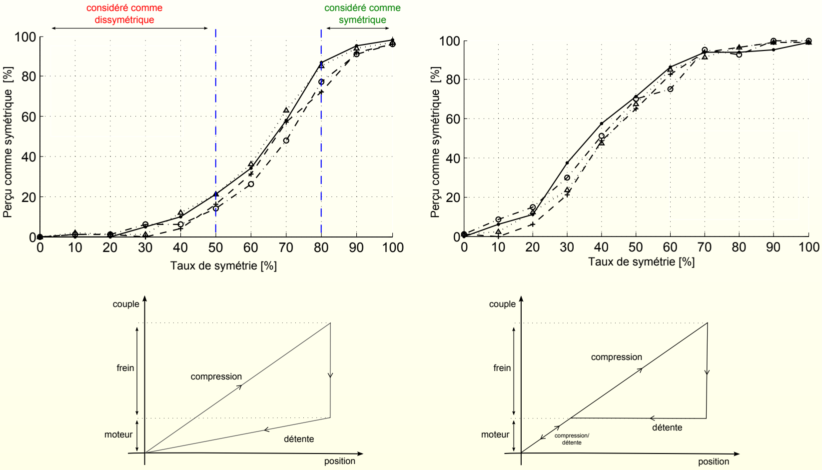

C. Rossa *et al.* - Perceptual evaluation of the passive/active torque and stiffness asymmetry of hybrid haptic device - Eurohaptics 2014

Results

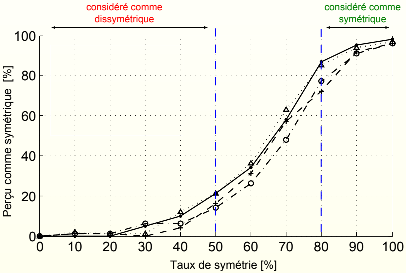

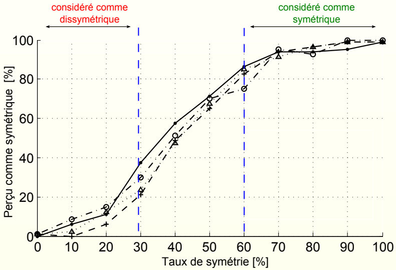

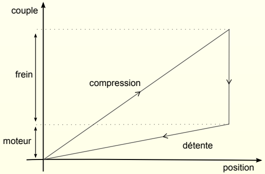

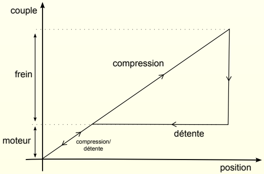

C. Rossa *et al.* - Perceptual evaluation of the passive/active torque and stiffness asymmetry of hybrid haptic device - Eurohaptics 2014

Conclusions

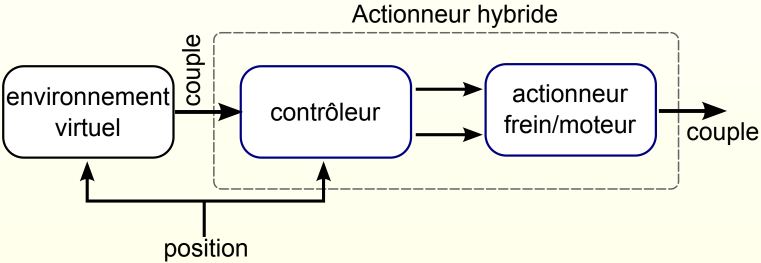

Conclusions

Design

Magnetostatic model for MR brakes
Evaluation and comparison of different geometries

Control

Controller independent of the VE
Allows for the application of the actuator in existent devices

Industrial transfer

Conclusions

Design

Magnetostatic model for MR brakes
Evaluation and comparison of different geometries

Control

Controller independent of the VE
Allows for the application of the actuator in existent devices

Industrial transfer

Conclusions

Design

Magnetostatic model for MR brakes
Evaluation and comparison of different geometries

Control

Controller independent of the VE
Allows for the application of the actuator in existent devices

Industrial transfer

Contributions

Journals

1. C. Rossa, A. Jaegy, J. Lozada et A. Micaelli, "*Design considerations for magnetohreological brakes*," Transactions on Mechatronics
2. C. Rossa, A. Jaegy, J. Lozada et A. Micaelli, "*Development of a mutilayered wide-ranged torque magnetorheological brake*," Smart Materials and Structures
3. C. Rossa, L. Eck, A. Micaelli et J. Lozada, "*On a novel torque detection technique for magnetorheological brakes*," Sensors Journal
4. C. Rossa, J. Lozada et A. Micaelli, "*Design and Control of a Dual unidirectional brake hybrid actuation system for haptic devices*,' Transactions on Haptics (soumis)

Contributions

Conferences

C. Rossa, J. Lozada et A. Micaelli,

1. "*Interaction power flow based control of a 1DOF haptic device*," Eurohaptics 2012
2. "*A new hybrid actuation approach for force feedback devices*," IROS 2012
3. "*Magnetic flux analysis on MR actuators can detect external force variation*," IEEE Sensors 2012
4. "*Stable haptic interaction using active and passive actuators*," ICRA 2013
5. "*Actionneur Hybride pour inteface à retour d'effort*", JCGE/SEEDS 2013
6. "*Perceptual evaluation of the passive/active torque and stiffness asymmetry of a hybrid haptic device*", Eurohaptics 2014

Patent activities

- C. Rossa, J. Lozada et A. Micaelli, "*Actionneur à actionnement hybride pour interface à retour de forces*"

Merci pour votre attention

Perspectives

Conception et commande

Prise en compte des frottements sec et visqueux
Compensation de l'hystérésis magnétique/asservissement en champ

Miniaturisation

Détection de couple par mesure de l'impédance électrique
Intégration d'un système de mesure de position

Interfaces multi-degrés de liberté

Maximisation de l'espace de travail des freins
Actionneur redondants

Perspectives

Conception et commande

Prise en compte des frottements sec et visqueux
Compensation de l'hystérésis magnétique/asservissement en champ

Miniaturisation

Détection de couple par mesure de l'impédance électrique
Intégration d'un système de mesure de position

Interfaces multi-degrés de liberté

Maximisation de l'espace de travail des freins
Actionneur redondants

Perspectives

Conception et commande

Prise en compte des frottements sec et visqueux
Compensation de l'hystérésis magnétique/asservissement en champ

Miniaturisation

Détection de couple par mesure de l'impédance électrique
Intégration d'un système de mesure de position

Interfaces multi-degrés de liberté

Maximisation de l'espace de travail des freins
Actionneur redondants

Contrôle sur l'énergie d'intéraction

L'observateur d'énergie est dénifit par :

$$E(n) = T \sum_{k=1}^{n} [\Gamma_{sb} + \Gamma_b^{**}] \, \dot{\theta}(k)$$

Redéfinition de $S(u)$

- Tant que l'énergie observée est positive :

$$S(u) = \beta(u)$$

- Tant que l'énergie d'intéraction est négative :

$$S(u) = 0$$

L'énergie injectée par l'échantillonnage est dissipée par le frein.

Flux de puissance

Le frein peut être désactivé si la vitesse et le couple ont le même signe.

- $S(u)$ Taux de participation du moteur
- $\Lambda(u)$ Taux non saturation de l'actionneur

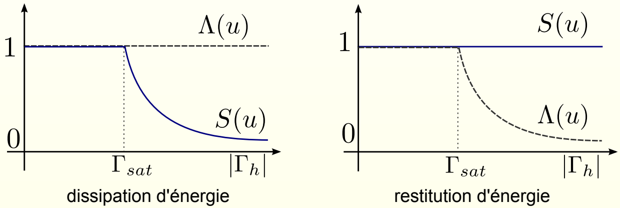

- Dissipation d'énergie : Frein + moteur
- Restitution d'énergie : Moteur

Réponse électromagnétique

- Réponse fréquentielle de la bobine

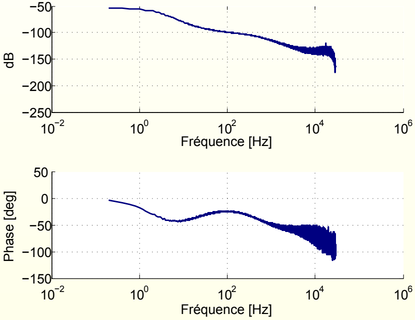

- La fréquence de coupure est de 18 Hz
- Suffisante pour les IHM ?

Réponse électromécanique

- Réponse à un échelon de tension en bouble ouverte
  - Temps de réponse 200 ms

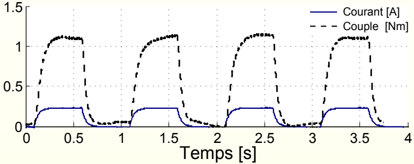

- Réponse à un échelon de courant avec contrôleur PI
  - Temps de réponse 30 ms